

RESEARCH

Open Access



Nicotinamide mononucleotide improves the ovarian reserve of POI by inhibiting NLRP3-mediated pyroptosis of ovarian granulosa cells

Yue Ma^{1†}, Weihua Nong^{2†}, Ou Zhong¹, Ke Liu¹, Siyuan Lei¹, Chen Wang¹, Xi Chen^{1*} and Xiaocan Lei^{1*}

Abstract

Background Premature ovarian insufficiency (POI) is a common clinical problem, but there is currently no effective treatment. NLRP3 inflammasome-induced pyroptosis is thought to be a possible mechanism of POI. Nicotinamide mononucleotide (NMN) has a certain anti-inflammatory effect, providing a promising approach for the treatment of POI.

Methods Thirty female Sprague Dawley rats were randomly divided into a control group ($n = 10$) and a POI group ($n = 20$). Cyclophosphamide (CTX) was administered for 2 weeks to induce POI. Then the POI group was divided into two groups: the CTX-POI group ($n = 10$), which was given saline; and the CTX-POI + NMN group ($n = 10$), which was given NMN at a dose of 500 mg/kg/day for 21 consecutive days. At the end of the study, the serum hormone concentrations of each group were determined, and each group was subjected to biochemical, histopathological, and immunohistochemical analyses. In the in vitro experiment, cell pyroptosis was simulated by using lipopolysaccharide (LPS) and nigrinin (Nig), and then KGN cells were treated with NMN, MCC950, and AGK2, and the levels of Nicotinamide adenine dinucleotide (NAD^+) and inflammatory factors Interleukin-18 (IL-18) and Interleukin-1 β (IL-1 β) in the cell supernatants were detected, and the levels of pyroptosis-related factors in the cells were determined.

Results In POI rats, NMN treatments can improve blood hormone levels and partially improve the number of follicles, enhance ovarian reserve function and ovarian index. The evidence is that the increase in NAD^+ levels and the activation of SIRT2 expression can reduce the expression of NLRP3, Gasdermin D (GSDMD), Caspase-1, IL-18, and IL-1 β in the ovary.

Conclusion NMN improves CTX-induced POI by inhibiting NLRP3-mediated pyroptosis, providing a new therapeutic strategy and drug target for clinical POI patients.

[†]Yue Ma and Weihua Nong contributed equally to this work.

*Correspondence:

Xi Chen

1987001730@usc.edu.cn

Xiaocan Lei

lxc2019000013@usc.edu.cn

Full list of author information is available at the end of the article



© The Author(s) 2024. **Open Access** This article is licensed under a Creative Commons Attribution-NonCommercial-NoDerivatives 4.0 International License, which permits any non-commercial use, sharing, distribution and reproduction in any medium or format, as long as you give appropriate credit to the original author(s) and the source, provide a link to the Creative Commons licence, and indicate if you modified the licensed material. You do not have permission under this licence to share adapted material derived from this article or parts of it. The images or other third party material in this article are included in the article's Creative Commons licence, unless indicated otherwise in a credit line to the material. If material is not included in the article's Creative Commons licence and your intended use is not permitted by statutory regulation or exceeds the permitted use, you will need to obtain permission directly from the copyright holder. To view a copy of this licence, visit <http://creativecommons.org/licenses/by-nc-nd/4.0/>.

Keywords Nicotinamide mononucleotide, Premature ovarian insufficiency, Pyroptosis

Background

Primary Ovarian Insufficiency (POI) is the term used to describe diminished ovarian function before age 40. It is typified by irregular menstruation, elevated gonadotropin levels (FSH > 25 U/L), and reduced fluctuations in estrogen (E_2) levels [1]. There is ample evidence that premature low estrogen status causes significant before-age harm to the long-term health of women, including the reproductive system, as well as adverse effects on bone, the cardiovascular and nervous systems, the genitourinary system, and sexual health [2, 3]. Patients may experience a significant reduction in quality of life. As such, long-term health management of POI patients is particularly important. There are several causes of POI, however, they can be generically categorized as immunological, iatrogenic, and genetic [4]. Ovarian damage is increasingly being caused by chemotherapy and radiation therapy [5]. Epidemiological studies show that the post-chemotherapy amenorrhea rate in women reaches 40–68% [6]. Cyclophosphamide (CTX), a type of alkylating or alkylating-like drug in the chemotherapy drug class, has been proven to have the strongest toxic effect on the ovaries, causing ovarian fibrosis, ovarian dysfunction, and oocyte loss [7]. CTX has recently been used as the main drug to create POI models in multiple studies [8–10].

Through an in-depth examination of the POI, it has been discovered that the manifestation and progression of POI are intricately linked to the presence of a chronic inflammatory state within the body [11, 12]. The malignant inflammatory factor profile alters the growth and functionality of ovarian cells, consequently causing a delay in follicle maturation and resulting in ovarian dysfunction [13, 14]. Pyroptosis, a type of inflammatory programmed cell death, has the potential to trigger severe inflammation and immune responses within the human body [15]. The NLR family pyrin domain containing 3 (NLRP3) inflammasome is one of the most extensively studied inflammasomes, given its ability to regulate the activation of Caspase-1 and facilitate the maturation and secretion of inflammatory cytokines, including interleukin-1 β (IL-1 β) and interleukin-18 (IL-18) [16, 17]. Additionally, previous studies have demonstrated that the NLRP3 inflammasome-induced cell pyroptosis plays a crucial role in the progression of POI [18], animal studies have demonstrated that excessive ROS generation induced by CTX in mouse ovaries activates the NLRP3 inflammasome, resulting in the heightened release of inflammatory mediators, including IL-1 β and IL-18, which contribute to ovarian dysfunction [19]. Nonetheless, interventions that restore the inflammatory status in the mouse ovaries facilitate the recovery of ovarian reserve function. Moreover, the

inhibition of NLRP3 delays the aging process of mouse ovaries and enhances fertility rates [20]. Thus, it is of paramount importance to investigate the impacts of NLRP3 inflammasome-mediated cell pyroptosis on POI women and its potential underlying mechanisms.

Nicotinamide mononucleotide (NMN) is synthesized by nicotinamide and 5'-phosphoribosyl-1-pyrophosphate (PRPP) in mammalian cells by the enzyme nicotinamide nucleotide transhydrogenase (NAMPT) and can be rapidly converted into Nicotinamide adenine dinucleotide (NAD^+) and exert its effects [21]. Meanwhile, previous studies have shown that NMN is also present in vegetables, fruits, and meats. There is evidence that systemic administration of NMN effectively enhances NAD^+ synthesis in various peripheral tissues, and increasing evidence supports the idea that NAD^+ can reduce inflammation levels in various organs of the body and improve body function [22–24]. Moreover, whereas administering NMN can enhance follicular growth in elderly ovaries by reducing follicular atresia and raising ovarian reserve, raising NAD^+ levels can lower ovarian inflammation, improve oocyte quality, and increase fertility [25]. Therefore, the purpose of this study is to successfully establish a CTX-induced POI rat model and determine whether NMN can improve the decline in ovarian reserve function induced by CTX-induced POI in rats by increasing NAD^+ levels and inhibiting NLRP3 inflammasome-mediated pyroptosis.

Materials and methods

Chemicals and reagents

CTX (batch number: 20050712, national drug name: H32020857) was purchased from Jiangsu Hengrui Pharmaceutical. NMN (batch number: XJY01231111) was obtained from Shenzhen Hygieia Biotech Co, Ltd.). Wright-Giemsa Stain solution (G1020), hematoxylin, eosin stain was purchased from Beijing Solarbio Science & Technology Co, Ltd (Beijing, China). HiScript III RT SuperMix (R323-01) for qRT-PCR (+gDNA wiper) was purchased from Vazyme Biotech Co, Ltd. Diaminobenzidine (DAB) chromogenic kit (ZLI-9018) was purchased from Beijing Zhongshan Jinqiao Biotechnology Co, Ltd. GSDMD Antibody (TA4012), and Anti- β -Tubulin (C66) mAb (M20005) were purchased from Abmart Pharmaceutical Technology Co., Ltd. (Shanghai, China). NLRP3 Rabbit pAb (A12694), Caspase-1 Rabbit pAb (A12575), SIRT2 Rabbit pAb (A12575), and IL-1 β Rabbit pAb (A16288) were purchased from Abclonal (Wuhan, China). IL-18 Polyclonal antibody (10663-1-AP), Horseradish peroxidase-conjugated goat anti-rabbit IgG (H+L) (SA00001-2), and biotinconjugated affinipure goat anti-rabbit IgG (H+L) (SA00004-2) were purchased from Protein Tech Group Inc. (Chicago, USA).

Trizol reagent (15596026 and 15596018) was purchased from Thermo Fisher Scientific (Waltham, 149 USA).

Animal

Thirty healthy female Sprague-Dawley (SD) rats, aged 8 weeks and weighing 200 ± 50 g, were purchased from Hunan Shrek Jingda Company (Changsha, China). All rats were acclimated to the environment for one week before the start of the experiment and underwent light-dark cycles for 12 h in a temperature-humidity-controlled chamber with food and water AD libitum. The animal experimentation procedures were conducted following the guidelines and were approved by the Laboratory Animal Welfare Ethics Committee of the University of South China (Approval NO: USC2020031602).

Experimental design

Following a week of adaptive feeding, the rats were randomly allocated into three groups: a control group ($n=10$), a Positive Outcome Index (POI) group ($n=10$), and a POI-NMN group ($n=10$). The latter two groups received protective drug intervention one week before the onset of the study. Specifically, the POI-NMN group initiated gavage administration of NMN (500 mg/kg/day in saline) [26] from the 8th day and continued for 42 consecutive days, as previously detailed. Conversely, the control group and the POI group were administered with saline via gavage. One week after the drug intervention, the POI group and NMN rats were injected with CTX (50 mg/kg

on day 1 and 8 mg/kg on day 2) [27]. intraperitoneally for 14 consecutive days to establish the POI model, while the control group rats were injected with saline intraperitoneally. The SD rats were monitored for vaginal smears 10 days before the end of the experiment to observe changes in the estrous cycle and preliminarily determine whether the model had been successfully established. Following the completion of the experiment, blood serum from each group was meticulously collected and analyzed to determine the hormone concentrations. Additionally, the rats and their ovaries were meticulously weighed, with the ovaries from each group being preserved for further investigation. A schematic diagram illustrating the study design is presented in Fig. 1.

Assessment of rat estrous cycles

Before the end of treatment, vaginal smears were performed at noon for ten consecutive days. The vagina of the rats was rinsed 2–3 times with 20ul of normal saline (0.9%NaCl), and the vaginal fluid was collected and applied to a slide, air-dried at room temperature, and stained using Swiss-Giemsa staining. The stages of the estrous cycle (proestrus, estrus, postestrus, and diestrus) were determined under a light microscope based on the number and proportion of vaginal epithelial cells and other cell types [28, 29]. The presence of nuclear epithelial cells characterized the proestrus phase, and the estrous phase primarily consisted of cornified squamous epithelial cells. The metestrus phase was characterized by the presence

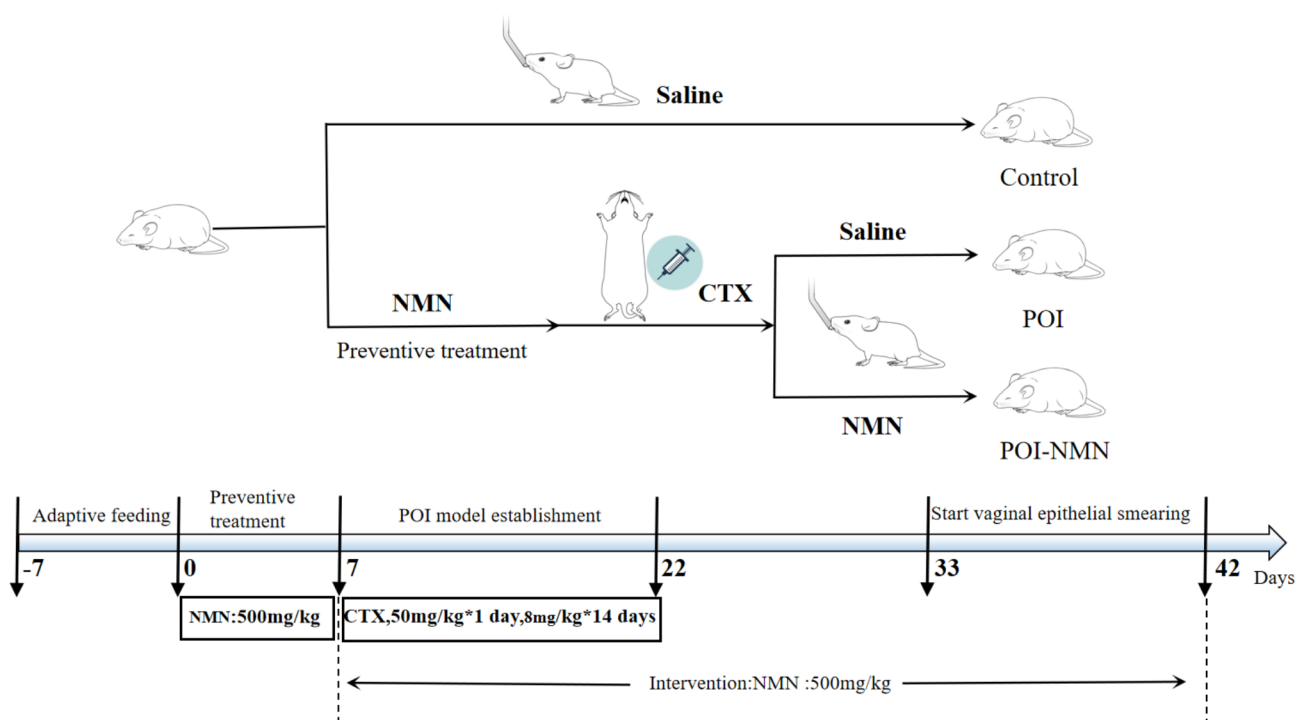


Fig. 1 Diagram of an experimental treatment for POI and POI-NMN rats

of leucocytes, nuclear epithelial cells, and cornified squamous epithelial cells, whereas the diestrus phase consisted almost entirely of leucocytes.

Ovarian morphological analysis and follicle count

One ovary from each rat was fixed in 4% formaldehyde for 24 h and then embedded in paraffin. The preparation of continuous 5 mm thick slices, hematoxylin-eosin staining, and check under the microscope. To quantify each number of ovarian follicles, every five consecutive slices, every four take a slice staining and analysis. According to the method of Pedersen and Peters (1968) [30], all levels of follicles (primordial follicles, primary follicles, secondary follicles, and atretic follicles) were counted in a double-blind method [31], and the obtained values were averaged as the follicle count of the ovary.

Ovarian index

Before euthanizing the rat, their body mass was recorded. Subsequently, following the isolation of the bilateral ovaries, the ovaries mass was measured to calculate the ovarian index. Ovarian Index = (ovarian mass [mg]/body mass [g]) × 100%.

Table 1 Primer sequences used for the qRT-PCR analysis

Target gene	Primer sequence(5'-3')	GeneBank Accession no.
RAT	F: GAGCTGGACCTCAGACAATGC	XM
NLRP3	R: AGAACCAATGCGAGATCCTGACAAC	006246457.4
RAT	F: ATGGCTCTGAATGGGATA	NM
GSDMD	R: CGGCACCAAGTTCTCCA	001400994.1
RAT	F: GACCGAGTGGTTCCTCAAG	NM
CASPASE-1	R: GACGTGTACGAGTGGGTGTT	012762.3
RAT	F: CGACCGAACAGCCAACGAATCC	NM
IL-18	R: GTCACAGCCAGTCCCTTACTTCAC	019165.2
RAT	F: CCCTTGTCGAGAATGGGCAG	NM
IL-1β	R: GACCAGAATGTGCCACGGTT	031512.2
RAT	F: CTCGCCTGCTCATCAACAAG	NM
SIRT2	R: GTCCTCCAGTCCCTTCTTCC	001399630
RAT	F: GAGTCCACTGGCGTCTTAC	XM
GAPDH	R: GAGGCATTGCTGATGATCTTGAG	032916238
HOMO	F: ATGCTGCTTCGACATCTCCT	XM
NLRP3	R: AACCAATGCGAGATCCTGAC	047443562.1
HOMO GSDMD	F: CAGAAGGGACGTGGTGTCC	NM
	R: AAGTGTTGAGGGCAGAACCC	001166237
HOMO	F: ATGGCTGCTGAACCAGTAGAAGAC	NM
IL-18	R: TCCGGGGTGCATTATCTTACAGTC	001562.4
HOMO	F: CCGACCACCTACAGCAAGG	NM
IL-1β	R: GGGCAGGGAACAGCATCTTC	000576.3
HOMO	F: CGCACGGCACCTTACACATC	NM
SIRT2	R: GGCTCTGACAGTCTTACACTTGG	001193286
HOMO GAPDH	F: GAGTCCACTGGCGTCTTAC	M33197.1
	R: GAGGCATTGCTGATGATCTTGAG	

Determination of hormone levels

After the rats were determined of hormone levels anesthetized, blood samples were collected by abdominal aortic puncture and serum was separated by centrifugation (3000×) for 15 min at 4 °C. The E2, FSH, and LH concentrations were measured in serum samples collected from rats in the diestrus phase using a commercial enzyme-linked immunosorbent assay (ELISA) kit (Beijing North Institute of Biotechnology Co., Ltd.).

RNA extraction and quantitative RT-PCR

The gDNA Removal and cDNA Synthesis SuperMix Kit reverse transcribe RNA to cDNA, according to the manufacturer's protocol, Real-time PCR analyses were performed with ChamQ Universal SYBR qPCR Master Mix (Q711-02; Vazyme, China) and Applied Biosystems QuantStudio 3 (Thermo Fisher Scientific, USA). GAPDH as control, level of gene expression is obtained by using the comparative CT method using Trizol reagent and ovarian tissue cells extracted total RNA, then use the TransScript One-Step gDNA Removal and cDNA short SuperMix Kit to RNA reverse transcription to cDNA, according to the manufacturer's protocol, Real-time PCR analyses were performed with ChamQ Universal SYBR qPCR Master Mix (Q711-02; Vazyme, China) and Applied Biosystems QuantStudio 3 (Thermo Fisher Scientific, USA). Gene expression levels were calculated using the comparative CT method with GAPDH as a control. The primer sequences used for amplification are shown in Table 1.

Immunohistochemistry (IHC) analysis

Ovaries were fixed in 4% formaldehyde, and embedded in paraffin, 5-um thick sections were washed with 3% hydrogen peroxide for 30 min, boiled 3 times in 0.1 M sodium citrate (pH 6.0) for antigen extraction, penetrated with 1% Triton X-100 and PBST for 30 min, and blocked with 5% bovine serum albumin for 45 min. Then, sections were incubated with the following rabbit primary antibodies SIRT2(1:100dilution), NLRP3(1:100dilution), IL-18(1:200dilution), IL-1β(1:200dilution), GSDMD(1:200dilution), and Caspase-1(1:100dilution) overnight at 4, with the corresponding secondary antibodies for 90 min at room temperature, and with HRP for another 45 min. The signal was visualized with DAB, where staining in tan indicated a positive result. Negative controls were obtained by replacing the primary antibody with PBST. Stained sections were observed under a light microscope.

Protein extraction and Western blot

The ovarian tissues or cells were incubated with Radio Immunoprecipitation Assay (RIPA) lysis buffer (R0100, Solarbio, Beijing, China) containing protease inhibitors on ice for 30 min, then under 4 °C at 12,000 RPM

centrifugal for 20 min. The supernatant was collected, and the protein concentration was determined using the BCA Protein Assay Kit (CW BIO) and denatured by boiling at 100 °C for 10 min. Denatured proteins were separated by 10% SDS-PAGE, electrophoresed and transferred to polyvinylidene fluoride (PVDF) membranes, and blocked for 2 h in PBST [phosphate buffered saline (PBS) containing 0.1% Tween-20] containing 5% skim milk powder. The blots were then incubated by primary rabbit monoclonal antibodies including SIRT2(1:1000dilution), NLRP3 (1:1000 dilution), Caspase-1 (1:1000 dilution), GSDMD (1:1000 dilution), IL-1 β (1:1000 dilution), and IL-18 (1:1000 dilution) overnight at 4 °C, followed by HRP-conjugated Affinipure goat anti-mouse IgG (H+L) (1:5000 dilution) or goat anti-rabbit IgG (H+L) (1:500 dilution) for 2 h at room. Beta-tubulin (1:5000 dilution) expression was used as a loading control. Finally, the blots were exposed to enhanced chemiluminescence (CW0049M, CW BIO) and a Tanon-5500 Chemiluminescence Imaging System was used to measure the chemiluminescence of protein bands. The intensity of specific bands was quantified using Image J analysis software (JAVA image processing program) (NIH, Bethesda, MD, USA).

Cell culture and treatment

KGN cells purchased from Zhejiang Meisen Cell Technology Co., Ltd were cultured routinely in DMEM medium (DMEM, Sigma, USA) containing 10% fetal bovine serum (FBS, Invitrogen 115 Gibco, USA) in a 5%CO₂ constant temperature cell incubator at 37°C. When the density of KGN cells reached 80–90%, the cells were harvested and seeded in a 6 cm dish. After 24 h of culture, the cells were cultured in a medium with or without LPS(1 μ g/ml, Sigma), Nig(10 μ mol/L, Med-Chem Express) [32], MCC950(100nmol/L, SparkJade) [33], AGK2(10 μ mol/L, Sigma) [34] and NMN(50 μ mol/L, Sigma) for 24 h.

Cell viability assay

A CCK-8 assay kit (BS350B, biosharp, China) determined the cell viability in 96-well plates according to the manufacturer's instructions. Each well of a 96-well plate should have a KGN cell density of 5 \times 10³ cells. The LPS group was treated with LPS at concentrations of 0, 0.1, 1, and 10 μ g mL⁻¹ and normal saline for 24 h, respectively. The LPS+Nig+NMN group was treated with normal saline, a mixture of LPS and Nig simultaneously, and the wells treated with LPS+Nig were treated with NMN at concentrations of 0, 10, 25, 50, and 100 μ M for 24 h. Then 10 μ L CCK-8 reagent was added to each well and then continuously incubated for 1–3 h at 37 °C in darkness. Finally, a PerkinElmer microplate reader was used to determine the absorbance.

NAD⁺ assay

Determination of NAD⁺ levels were conducted by using a Coenzyme I NAD (H) content test kit (A114-1-1; Nanjing Jiancheng, China) according to the manufacturer protocol. In each independent experiment, at least 5 \times 10⁶ cells were used for total NAD⁺ extraction according to the manufacturer's protocol. Use the enzyme standard instrument (Bio-Tek Instruments, Inc., Winooski, VT, USA) to measure absorbance for 570. Finally, according to the directions of the formula calculate each the NAD⁺ concentration of the sample.

Enzyme-linked immunosorbent assay (ELISA)

IL-18 and IL-1 β in the culture supernatant were detected by ELISA kits from Ruixinbio (Quanzhou, China), following the manufacturer's instructions.

Lactate dehydrogenase (LDH) activity detection

The LDH concentration in the KGN cell supernatant was measured using an LDH assay kit (Cat# C0016, Beyotime, Shanghai, China) and according to the manufacturer's instructions. The absorbance at 450 nm was measured and the LDH content of each supernatant was investigated. The LDH level in the control group was fixed at 100%, and the LDH concentration in the other groups was normalized to match.

Statistical analysis

Statistical analysis was conducted using GraphPad Prism 8.0.1 (GraphPad Software, San Diego, California) and SPSS 18.0 software (IBM, Chicago, IL, USA). The data are presented as means \pm standard deviation (SD) and were analyzed using one-way ANOVA. A probability of $p < 0.05$ was considered statistically significant. Each experiment was independently performed at least three times.

Result

Effects of NMN intervention on hormone levels and estrous cycle in POI rats

The main manifestations of ovarian function are endocrine function and reproductive function. Ovarian endocrine dysfunction can lead to estrous cycle disorder in rats. Serum levels of FSH, LH, and E2, as well as the estrous cycle, were examined to examine how NMN affected POI rat performance. During their estrous cycle, SD rats typically go through four or five days of proestrus, estrus, postestrus, and interestrus. As can be seen, proestrus was marked by the presence of nucleated epithelial cells (green arrows), and the estrus phase was primarily composed of keratinized squamous epithelial cells (red arrows). Control rats exhibited regular estrus cycles lasting four to five days. The estrus phase is characterized by leukocytes, nuclear epithelial cells, and keratinized squamous epithelial cells, whereas the diestrus phase consists almost

exclusively of leukocytes (blue arrows). Rats in the POI group showed estrus cycle disorder after CTX induction, were in estrus for a long time, and did not even appear to have a complete estrus cycle. After administration of

NMN, the abnormal estrous cycle gradually recovered. (Figure 2A-C) We next evaluated hormone levels, by the ELISA method, the expression levels of E2, FSH, and LH in serum were detected. The results showed that the

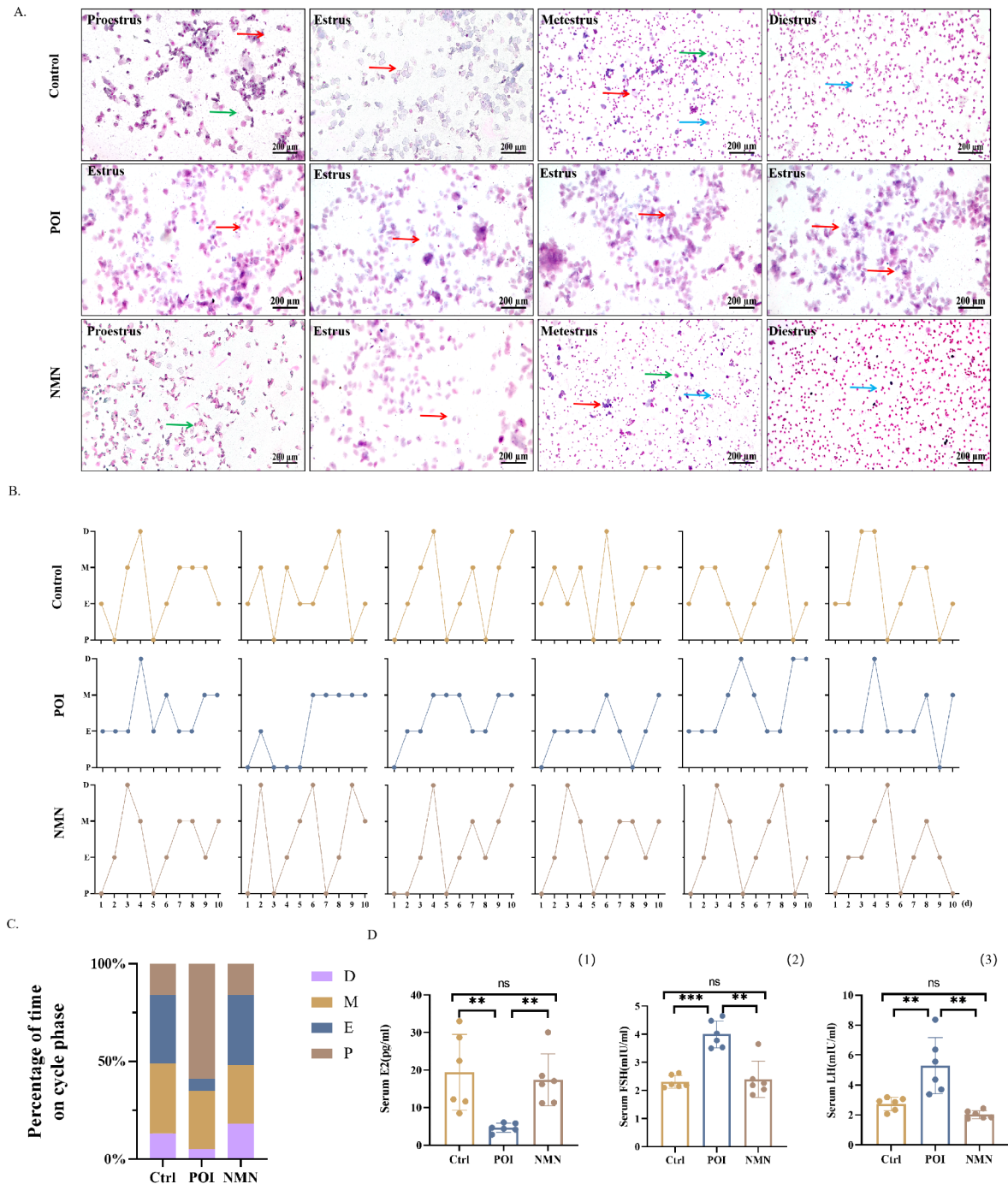


Fig. 2 NMN intervention improves POI rats' estrous cycle and endocrine function. **A)** Cytological evaluation of vaginal smears ($n=6$ rats per group, day 33–42). **B)** Representative estrous cycles. **C)** Analyze the percentage of time spent in each estrous cycle quantitatively ($n=6$ rats per group). **D)** Indicators of serum hormones include estradiol (E2) (1) follicle-stimulating hormone (FSH) (2) and luteinizing hormone (LH) (3) ($n=6$ rats per group). The data of C are presented as mean \pm standard deviation (SD). * $p < 0.05$, ** $p < 0.01$, *** $p < 0.001$. ns: no statistically significant difference

E2 level was lower in the POI group than in the control group, while the FSH and LH levels were higher in the POI group. After NMN intervention, the hormone levels were restored to similar levels as those in the control group. In conclusion, the disrupted estrous cycle and abnormal serum hormone levels gradually recovered after the application of NMN. (Figure 2D)

Effects of NMN intervention on ovarian morphology and reserve function in rats

Because the number of follicles in the ovary more directly reflects the ovarian reserve function, the size of the ovary is also an important factor in reflecting ovarian function, so to explore whether NMN intervention can prevent the decline of ovarian function caused by CTX, we compared

the ovarian index of each group of rats and observed the morphological changes of the ovaries in each group and counted the number of follicles at different stages. The findings revealed that the ovarian volume in the CTX-induced POI rats was diminished, and the ovarian index decreased. (Figure 3A and B) Microscopic examination demonstrated a decreased count of primordial, primary, and secondary follicles, concomitant with an elevated number of atretic follicles. After NMN intervention, the volume of the ovary was significantly restored, the number of primordial follicles was significantly increased, and the number of primary and secondary follicles was like that of the CTX group, while the number of atretic follicles was significantly reduced. (Figure 3C and D). Nonetheless, the count of primordial follicles in the NMN-treated group

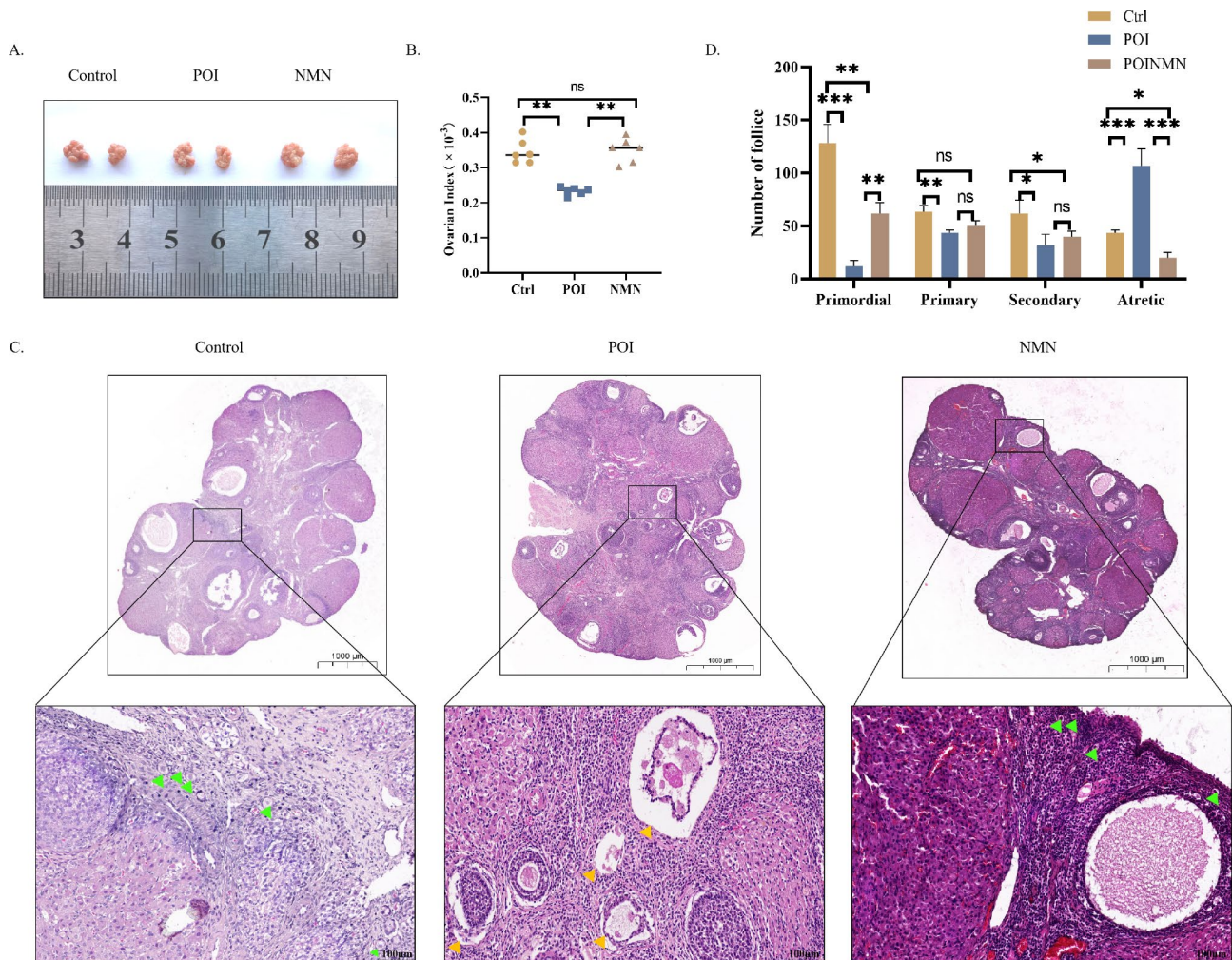


Fig. 3 NMN intervention can improve ovarian reserve function and ovarian morphology in rats with POI. **A)** Representative appearance of ovaries; **B)** Ovary weight and ovary index (n=6 rats per group); **C)** Representative HE staining images of ovarian tissue, green arrows, primordial follicle, yellow arrows, atretic follicle; **D)** Follicle counts for each stage of development (n=6 rats per group). *p<0.05, **p<0.01. ns: no statistically significant difference

remained lower compared to that in the control group. Therefore, these findings suggest that NMN can partially improve the decline in ovarian reserve function in POI rats induced by CTX.

NMN treatment inhibits the pyroptosis of ovarian in POI rats

NLRP3 inflammasome-induced pyroptotic cell death (proptosis) is considered a possible mechanism of POI, to confirm that pyroptosis is related to the progression of POI and that NMN intervention can alleviate the level of pyroptosis in POI, we detected the mRNA expression levels of NLRP3, Caspase-1, GSDMD, IL-1 β , and IL-18 in ovarian tissue by qRT-PCR, as shown in Fig. 4B. Compared with the control group, the mRNA expression levels of NLRP3, Caspase-1, GSDMD, IL-1 β , and IL-18 were significantly upregulated in the POI rats treated with CTX,

and they were significantly downregulated after NMN intervention. Western blotting and immunohistochemical analysis also confirmed this result. (Figure 4A and C) Thus, NMN intervention has a protective effect on the pyroptosis of granulosa cells in the ovaries of POI rats induced by CTX.

NMN intervention improves ovarian dysfunction by increasing the level of NAD⁺ to activate SIRT2

Sirtuin 2 (SIRT2) is a metabolic sensor and NAD⁺-dependent deacetylase. Acetylation of NLRP3 facilitates NLRP3 inflammasome formation and activation. As a result, we measured the amount of NAD⁺ in the ovaries of the three groups of rats, and the results showed that the level of NAD⁺ in the POI group was significantly lower than that in the control group, and the level of NAD⁺ was increased considerably after NMN intervention. (Fig. 5A) Therefore,

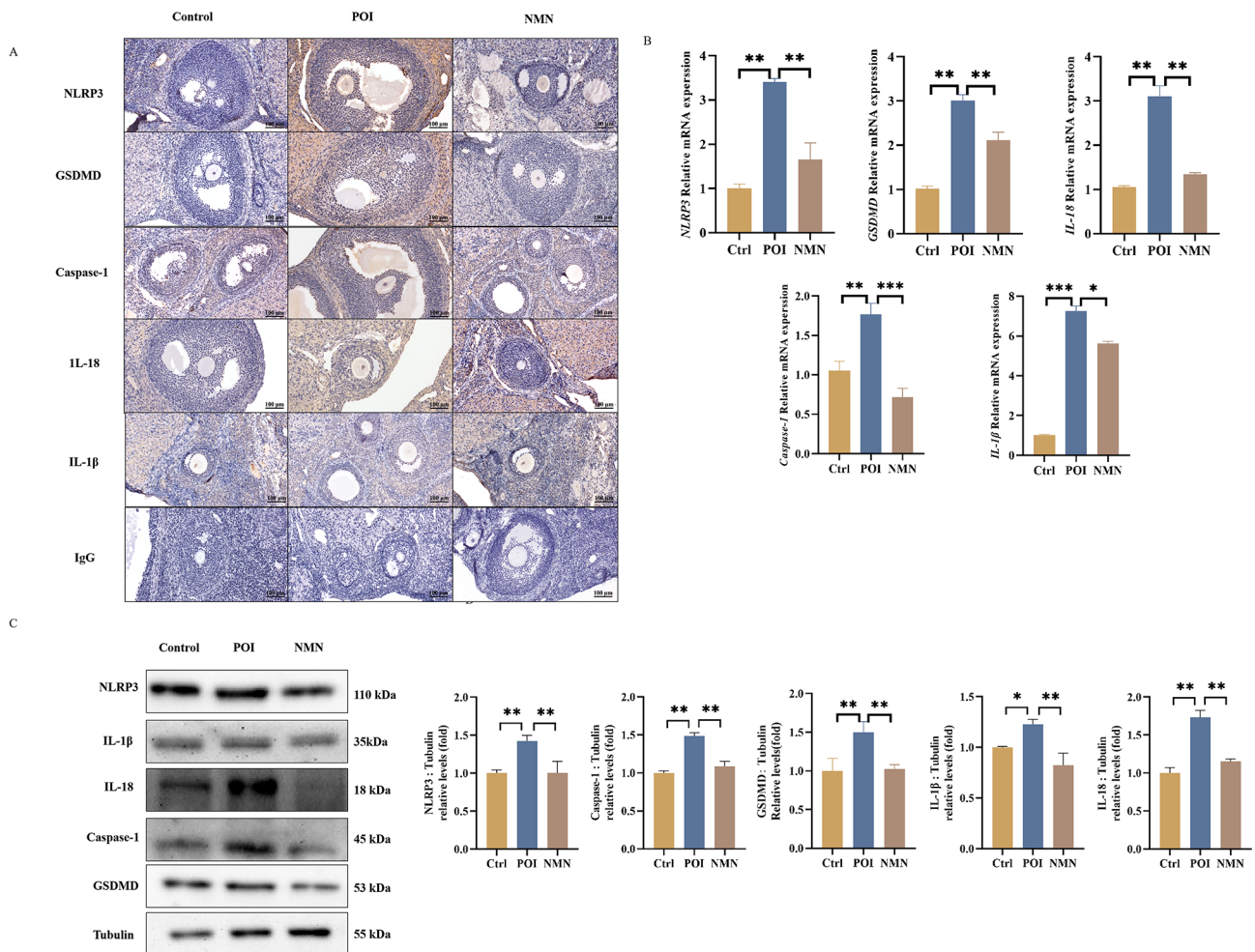


Fig. 4 NMN intervention inhibits the pyroptosis of ovarian in POI rats. **A**) Immunohistochemical analysis of NLRP3, GSDMD, Caspase-1, IL-1 β , and IL-18 expression in the ovaries; **B**) The mRNA levels of NLRP3, GSDMD, Caspase-1, IL-1 β , and IL-18 analyzed by qRT-PCR. GAPDH was used as control; **C**) Expression of NLRP3, GSDMD, Caspase-1, IL-1 β , and IL-18 was measured by Western blot, β -tubulin served as the loading control; **D**) Relative protein expression of NLRP3, GSDMD, Caspase-1, IL-1 β , and IL-18 were quantified by ImageJ software and normalized to β -tubulin ($n = 3$ rats per group); data are presented as mean \pm standard deviation (SD). * $p < 0.05$, ** $p < 0.01$

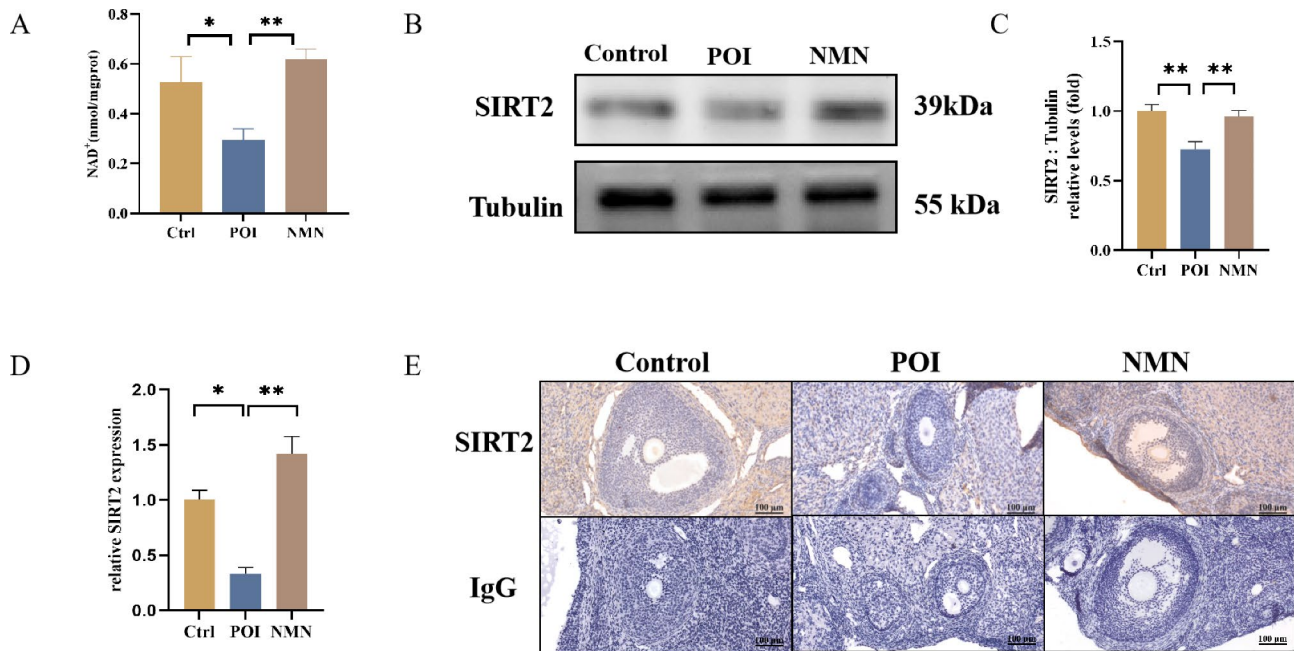


Fig. 5 NMN can increase NAD⁺ levels and restore the expression of SIRT2 in POI rats. **A**) Determination of NAD⁺ content; **B**) Protein expression of SIRT2 in the ovaries was determined using western blot analysis, β -tubulin served as the loading control; **C**) Relative protein expression of SIRT2 was quantified by ImageJ software and normalized to β -tubulin ($n=3$ rats per group); **D**) The mRNA levels of SIRT2 analyzed by qRT-PCR, GAPDH was used as control; **E**) Immunohistochemical analysis of SIRT2 expression in the ovaries; data are presented as mean \pm standard deviation (SD). * $p < 0.05$, ** $p < 0.01$

we further used qRT-PCR, WB, and IHC to detect the expression of SIRT2. The results showed that the expression of SIRT2 mRNA in the POI group was significantly lower than in the control group, and the mRNA expression was upregulated after NMN intervention. (Fig. 5D) SIRT2 protein expressions were shown to be considerably lower in the POI group compared to the control group, according to Western blot analysis. Following NMN administration, there was an increase in the expression of the proteins. (Figure 5B-C) The results of immunohistochemistry showed the same outcome. (Fig. 5E)

Intervention with NMN can inhibit the levels of inflammation and cell pyroptosis in KGN cells

To further explore its molecular mechanism, we induced necroptosis in KGN cells by adding LPS and Nig. We treated KGN cells with different concentrations of LPS and measured cell viability. The CCK8 results showed that KGN cell viability decreased dose-dependently, so we selected 1 μ g/ml of LPS for subsequent cell experiments. Similarly, we selected 50 μ mol/L of NMN for subsequent experiments. (Figure S1A-C) First, we detected the levels of IL-18 and IL-1 β in the cell culture supernatants and the release of LDH in each group of KGN cells. We found that the levels of IL-18 and IL-1 β released by KGN cells after LPS+Nig treatment were significantly increased, while those levels were significantly decreased after treatment with MCC950 or NMN. (Fig. 6A) Meanwhile, the LDH release of KGN cells treated with LPS+Nig was increased

considerably, while the LDH release of KGN cells treated with NMN or MCC950 was significantly reduced. (Fig. 6E) It is worth noting that there was no statistically significant difference between NMN and MCC950. Based on these results, we can preliminarily prove that NMN treatment can improve the exogenous high inflammatory state of KGN cells and inhibit KGN cell pyroptosis. To further confirm the effect of NMN on the process of cell pyroptosis, the expression levels of pyroptosis-related factors NLRP3, GSDMD, Caspase-1, IL-18, and IL-1 β at the mRNA and protein levels were detected by qRT-PCR and Western Blot. The results showed that the mRNA expression levels of NLRP3, GSDMD, Caspase-1, IL-18, and IL-1 β in KGN cells treated with LPS+Nig were significantly increased. After intervention with NMN and MCC950, the expression of both pyroptosis and inflammation factors improved. (Fig. 6B) The results from Western Blot and qRT-PCR were consistent, (Fig. 6C-D) and these findings were also corroborated by animal-level results, further indicating that NMN can regulate pyroptosis and inflammation factor expression by inhibiting NLRP3.

NMN enhances SIRT2 activation by elevating NAD⁺ levels to ameliorate KGN cell pyroptosis levels

To further verify whether NMN can inhibit pyroptosis by activating SIRT2, we added AGK2 inhibitor to cells after LPS+Nig treatment to suppress SIRT2 activity, based on previous studies and literature. We selected 10 μ mol/L AGK2 for subsequent experiments [34]. We measured the

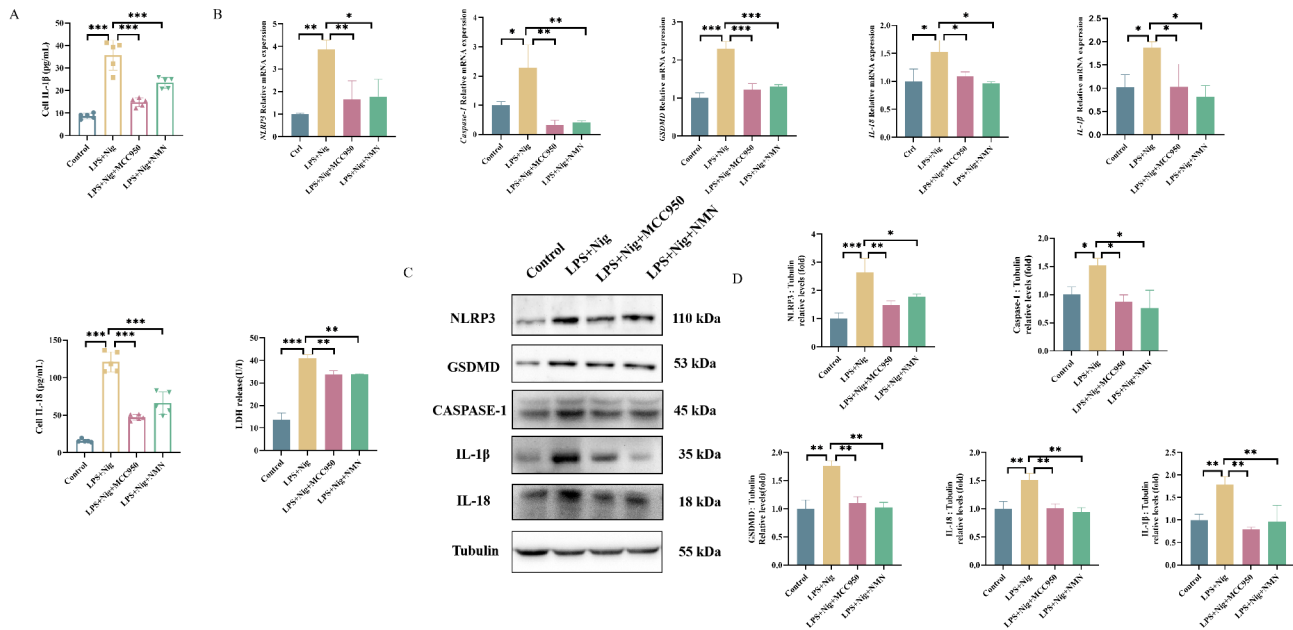


Fig. 6 NMN intervention downregulates the expression of pyroptosis factors induced by LPS and Nigrin trypanosomiasis in KGN cells. **A)** The levels of IL-1 β and IL-18 in the supernatants were analyzed by enzyme-linked immunosorbent assay (ELISA); **B)** Relative mRNA expression of NLRP3, GSDMD, Caspase-1, IL-1 β , and IL-18 in the KGN cells, analyzed using qRT-PCR; **C)** Protein expression of NLRP3, GSDMD, Caspase-1, IL-1 β , and IL-18 in the KGN cells was determined using western blot analysis, β -tubulin served as the loading control; **D)** Relative protein expression of NLRP3, GSDMD, Caspase-1, IL-1 β , and IL-18 in the KGN cells were quantified by ImageJ software and normalized to β -tubulin; **E)** The release of LDH in KGN cell detected by LDH activity assays. Data are presented as mean \pm standard deviation (SD). * $p < 0.05$, ** $p < 0.01$, *** $p < 0.001$

levels of NAD⁺ in each group of cells and found that the NAD⁺ level in KGN cells treated with LPS+Nig was significantly lower than that in the control group. After being given NMN, the NAD⁺ level was reversed. (Fig. 7A) qRT-PCR and Western Blot were used to detect the expression of SIRT2 mRNA and protein in each group of cells. Compared with the control group, the expression of SIRT2 mRNA was downregulated after LPS+Nig intervention. After being given NMN, the expression of SIRT2 mRNA was upregulated. After adding AGK2, the expression of SIRT2 mRNA was downregulated again. (Fig. 7D) The WB results were consistent with the trend of mRNA expression. (Figs. 7B-C) Based on these results, we concluded that NMN can activate SIRT2 by increasing NAD⁺ levels. Subsequently, we detected the expression of NLRP3, Caspase-1, GSDMD, IL-18, and IL-1 β mRNA and protein by qRT-PCR and Western Blot in each group of cells to see that compared with the control group, the mRNA expression of NLRP3, Caspase-1, GSDMD, IL-18, and IL-1 β was significantly upregulated after LPS+Nig intervention. After adding NMN, the mRNA expression was upregulated again. However, after SIRT2 was inhibited, the mRNA expression of NLRP3, caspase-1, GSDMD, IL-18, and IL-1 β was significantly upregulated again. (Fig. 7E) The WB results were consistent with the mRNA results. (Fig. 7F-J). Meanwhile, we detected the release of LDH in the supernatants of KGN cells in different treatment groups, and the results showed that the release of LDH in

cells treated with LPS+Nig was significantly higher than that in the control group. After adding NMN, the release of LDH was reduced, but it increased again after SIRT2 was inhibited. (Fig. 7H) In summary, supplementing NMN can activate the activity of SIRT2 in KGN cells to inhibit the level of NLRP3-mediated cell pyroptosis.

Discussion

POI is a globally prevalent disease, the pathogenesis of which remains predominantly obscure. It is potentially associated with age, genetic predispositions, immune system dysregulation, iatrogenic influences, or environmental triggers [35]. Currently, there is no satisfactory treatment for POI patients in clinical practice, and hormone replacement therapy is often used for symptomatic treatment [36]. With the occurrence of lifestyle changes and other factors, the probability of young women developing cancer escalates year after year [37]. Although early diagnosis and advancements in tumor technology can enhance the survival rate of young women during their childbearing years, chemotherapy and other cancer treatment modalities can deplete ovarian reserve and impair ovarian function, ultimately leading to the occurrence of POI [38–40]. Therefore, investigating the potential mechanisms by which chemotherapy leads to ovarian damage is essential for the advancement of POI research. This study demonstrates that CTX can induce ovarian dysfunction, and NMN intervention can ameliorate ovarian damage.

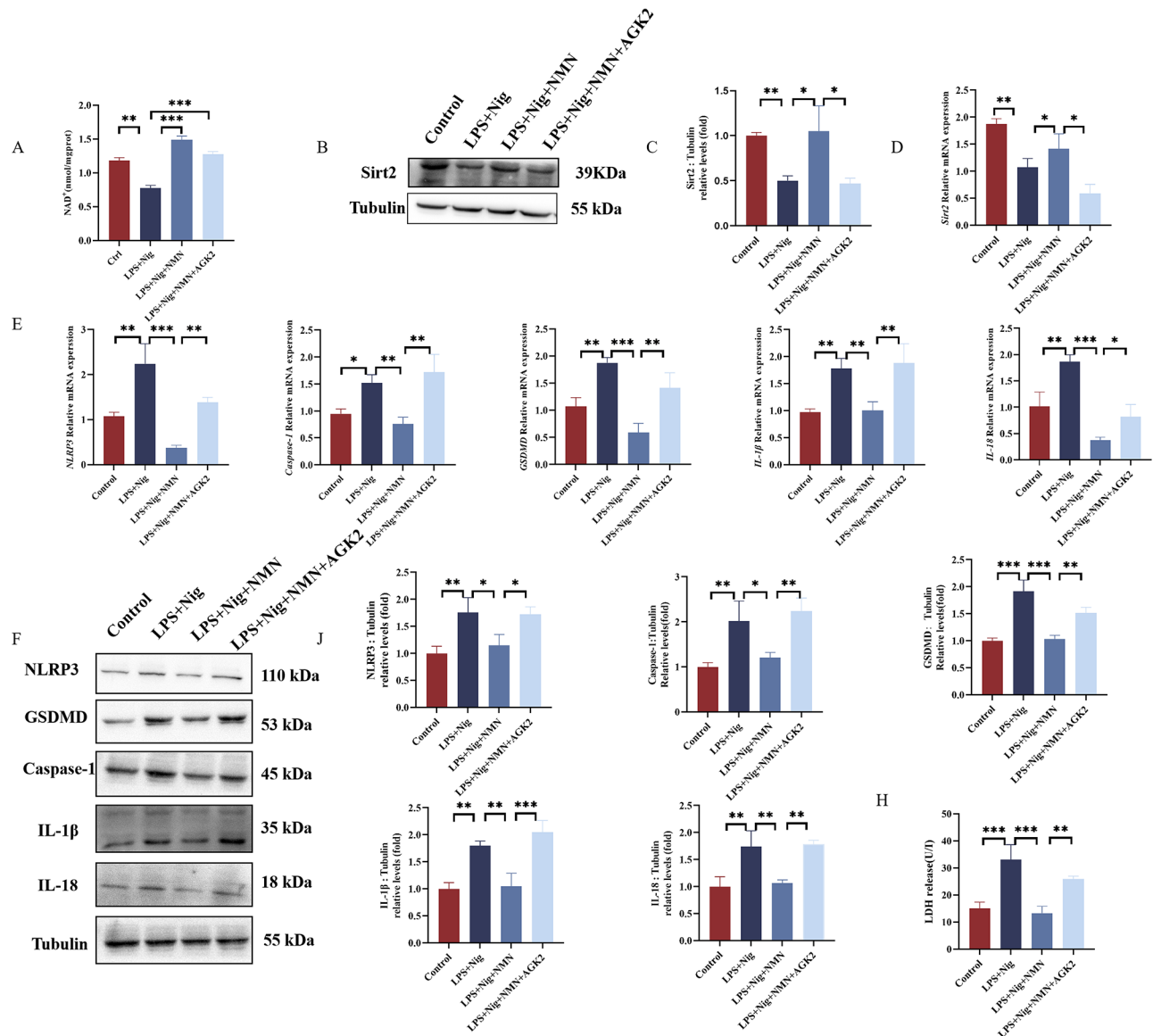


Fig. 7 NMN enhances SIRT2 activation by elevating NAD⁺ levels to ameliorate KGN cell pyroptosis levels. **A)** Determine the content of NAD⁺ in KGN cells. **B)** Protein expression of SIRT2 in the KGN cells was determined using western blot analysis, β -tubulin served as the loading control; **C)** Relative protein expression of SIRT2 in the KGN cells was quantified by ImageJ software and normalized to β -tubulin; **D)** Relative mRNA expression of SIRT2 in the KGN cells analyzed using qRT-PCR; **E)** Relative mRNA expression of NLRP3, GSDMD, Caspase-1, IL-1 β , and IL-18 in the KGN cells, analyzed using qRT-PCR; **F)** Protein expression of NLRP3, GSDMD, Caspase-1, IL-1 β , and IL-18 in the KGN cells was determined using western blot analysis, β -tubulin served as the loading control; **J)** Relative protein expression of NLRP3, GSDMD, Caspase-1, IL-1 β , and IL-18 in the KGN cells were quantified by ImageJ software and normalized to β -tubulin; **H)** The release of LDH in KGN cell detected by LDH activity assays. Data are presented as mean \pm standard deviation (SD). * $p < 0.05$, ** $p < 0.01$, *** $p < 0.001$

Furthermore, we have elucidated that CTX-induced POI is intricately associated with pyroptosis, underscoring the protective function of NMN on ovarian function.

CTX is an alkylating drug that is widely used in anti-cancer therapy and is also one of the drugs with the highest risk of POI [41]. In a large study of cancer survivors, the risk of POI in patients receiving alkylating chemotherapy was increased by 9.2 times, and the risk of POI in women receiving alkylating chemotherapy and radiation

was increased by 27 times [42, 43]. Similarly, animal experiments have shown that CTX can cause disorders in hormone secretion, damage to the ovary structure, and a decline in fertility in rats [44, 45]. Our research results are consistent with previous research results, where CTX-induced POI rat models showed elevated serum FSH and LH levels, decreased E2 levels, lower ovarian index, disrupted estrous cycle, and an increase in the number of atretic follicles, and a decrease in the number of atretic

follicles. In recent years, natural drugs have attracted widespread attention from both domestic and foreign research and clinical trials as effective, multi-pathway, multi-target drugs [46]. NMN is one of these drugs, which can be widely used as a dietary supplement and cosmetics in daily life [47]. It serves as a crucial intermediate for NAD⁺ in the body, capable of being rapidly converted into NAD⁺ and exerting its functions, including oxidative stress, DNA damage, neurodegenerative diseases, and inflammatory responses [23, 48]. In the context of reproductive research, several studies have demonstrated that supplementing with NMN can restore the levels of NAD⁺ in aged or obese mouse oocytes, improving their quality and fertility, as well as improving mitochondrial function, lowering ROS levels, slowing down oocyte aging, and encouraging subsequent embryo development [25, 49–51]. Meanwhile, NMN has also been shown to have the potential to save declining ovarian reserve through long-term treatment [52]. Our findings are largely in agreement with those from previous studies on NMN, which have shown that after NMN treatment, the serum sex hormone levels of rats return to normal, ovarian indices increase, primordial follicles increase, and atretic follicles decrease [52, 53]. These results indicate that NMN can partially restore ovarian damage induced by CTX.

Widely recognized, unregulated chronic inflammation results in the dysfunction of female ovarian function, with the NLRP3 inflammasome being the most extensively studied type of inflammasome [54, 55]. It is widely believed that granulosa cell pyroptosis, mediated by the NLRP3, is intricately linked to POI [11, 18]. Previous studies have shown that the expression of NLRP3, Caspase-1, and IL-1 β in granulosa cells of POI patients is significantly increased. In animal experiments, giving MCC950 to inhibit the activation of NLRP3 inflammasome resulted in the same effect as NLRP3^{-/-} mice, which can delay ovarian aging in female mice and prolong reproductive ability [20]. Similarly, in the CTX-induced POI rat model, ovarian dysfunction and fibrosis were caused by the activation of the NLRP3 inflammasome. Our results validate the relationship between NLRP3 inflammasome and POI consistent with previous findings [56, 57]. Meanwhile, NMN, a natural anti-inflammatory agent, can alleviate inflammation and chronic diseases [58]. Studies have shown that NMN can alleviate cognitive impairment caused by sepsis-induced inflammation, and supplementing with NMN can significantly reduce inflammation in mice and alleviate colitis, improving survival rates [59, 60]. Additionally, NMN supplements can reduce bone damage induced by aluminum through the inhibition of the necroptosis pathway mediated by thioredoxin interacting protein (TXNIP)-NLRP3 inflammasome [61], as we have validated both in vivo and in vitro experiments showing that supplementing with NMN can improve NLRP3-mediated cell necroptosis

levels, with an effect similar to that of MCC950, and partially restored ovarian reserve function in CTX-induced POI rats, suggesting a potential relationship between POI and necroptosis and showing the benefits of NMN for the ovary. NMN exhibits similar effects on the cellular level as MCC950, indicating that it inhibits the activation of the NLRP3 inflammasome in ovarian granulosa cells.

SIRT2, as a member of the Sirtuins family, is an NAD⁺-dependent deacetylase, and numerous studies have shown that the level of NAD⁺ can affect the activity of SIRT2 [62, 63]. Our previous research has demonstrated that upregulating the expression of SIRT2 can regulate the expression of glycolytic rate-limiting enzymes, improving ovarian function [34]. Additionally, NAD⁺ can enhance the antioxidant capacity of cells and increase the activity of SIRT2 under basal conditions, which can be partially reversed after inhibiting SIRT2 with AGK2 [64]. Similarly, we found that NAD⁺ synthesis was decreased in POI rats, and SIRT2 expression was lower in the ovaries. However, when NMN was given to increase NAD⁺ levels, SIRT2 expression increased in the ovaries, suggesting that SIRT2 may play a role in the ovaries. On the other hand, as an important deacetylase, studies have shown that SIRT2 can deacetylate NLRP3 in vitro, inhibit NLRP3 inflammasome activation, reverse aging-related inflammation and insulin resistance, and SIRT2 can also inhibit NLRP3 inflammasome activation in cardiac tissue, slowing the progression of dilated cardiomyopathy [65, 66]. In our study, the expression of SIRT2 increased, while the expression of NLRP3-mediated pyroptosis-related factors decreased after SIRT2 was expressed. However, AGK2 could inhibit SIRT2 in the experimental process, which offset the benefits of NMN in suppressing NLRP3 inflammasome activation in granulosa cells. It is worth noting that these results are still in the initial stages and need further investigation. In summary, inhibiting NLRP3-mediated granulosa cell pyroptosis is one of the key mechanisms by which NMN protects ovarian reserve in CTX exposure.

In conclusion, the results of this study demonstrate that NMN can protect female rat ovaries from ovarian damage induced by CTX. Both in vitro and in vivo experiments show that NMN can alleviate the decline in ovarian reserve function induced by CTX by increasing NAD⁺ levels and activating SIRT2 to inhibit NLRP3-mediated cell pyroptosis. This finding further confirms the defensive mechanism of NMN against the reproductive damage caused by CTX. Additionally, this increases the evidence supporting NMN as a feasible treatment for female reproductive dysfunction.

Abbreviations

POI	Premature ovarian insufficiency
CTX	Cyclophosphamide
FSH	Follicle stimulating hormone
GCs	Granulosa cells

E2	Estradiol
LH	Luteinizing hormone
IL-1 β	Interleukin-1 β
IL-18	Interleukin-18
LPS	Lipopolysaccharide
NLRP3	NOD-like receptor thermal protein domain associated protein 3
NAD ⁺	Nicotinamide adenine dinucleotide
NAMPT	Nicotinamide nucleotide transhydrogenase
NMN	Nicotinamide mononucleotide
Nig	Nigricin
HE	Hematoxylin and Eosin
SD	Sprague–Dawley
RIPA	Radio Immunoprecipitation Assay Lysis
TBST	Tris Buffered Saline with Tween [®] 20
PVDF	Polyvinylidene Fluoride
GAPDH	Glyceraldehyde-3-phosphate dehydrogenase
PBS	Phosphate-buffered saline
HRT	Estrogen replacement therapy
TLRs	Toll-like receptors

Supplementary Information

The online version contains supplementary material available at <https://doi.org/10.1186/s13048-024-01534-w>.

Supplementary Material 1

Supplementary Material 2

Author contributions

Y. M., W.H.N., and X.C.L. designed the study. The experiments were performed by Y.M., W.H.N., and O.Z.; Material preparation, data collection, and analysis were performed by S.Y.L., C.W., and K.L.; X.C., X.C.L. responsible for the comprehensive technical support; The first draft of the manuscript was written and revised by Y.M., W.H.N., and X.C.

Funding

This study was supported by the National Natural Science Foundation of China (82101720); The 2022 Scientific Research and Technology Development Program of Baise City (20224124); and the National Training Program of Innovation and Entrepreneurship for Undergraduates (S20232055214).

Data availability

No datasets were generated or analysed during the current study.

Declarations

Ethics approval and consent to participate

This study was approved by the Experimental Animal Welfare Ethics Review Committee of South China University of Technology.

Consent for publication

Not applicable.

Competing interests

The authors declare no competing interests.

Clinical trial number.

Not applicable.

Author details

¹Institute of Clinical Anatomy & Reproductive Medicine, Department of Histology and Embryology Hengyang Medical School, University of South China Hengyang, 421001 Hunan, China

²Key Laboratory of Research on Clinical Molecular Diagnosis for High Incidence Diseases in Western Guangxi, Department of Obstetrics and Gynecology, Department of Reproductive Medicine Center, Affiliated Hospital of Youjiang Medical University for Nationalities, Baise 533000, Guangxi, China

Published online: 26 November 2024

References

- Nash Z, Davies M. Premature ovarian insufficiency. *BMJ*. 2024;e077469.
- Sullivan SD, Sarrel PM, Nelson LM. Hormone replacement therapy in young women with primary ovarian insufficiency and early menopause. *Fertil Steril*. 2016;106:1588–99.
- Tsiligiannis S, Panay N, Stevenson JC. Premature ovarian insufficiency and long-term Health consequences. *CVP*. 2019;17:604–9.
- Ishizuka B. Current understanding of the etiology, Symptomatology, and Treatment options in premature ovarian insufficiency (POI). *Front Endocrinol (Lausanne)*. 2021;12:626924.
- Zhao P, Guo C, Du H, Xiao Y, Su J, Wang X, et al. Chemotherapy-induced ovarian damage and protective strategies. *Hum Fertility*. 2023;26:887–900.
- Spears N, Lopes F, Stefansdottir A, Rossi V, De Felici M, Anderson RA, et al. Ovarian damage from chemotherapy and current approaches to its protection. *Hum Reprod Update*. 2019;25:673–93.
- Morgan S, Anderson RA, Gourley C, Wallace WH, Spears N. How do chemotherapeutic agents damage the ovary? *Hum Reprod Update*. 2012;18:525–35.
- Hu Y, Zhong R, Guo X, Li G, Zhou J, Yang W, et al. Jinfeng pills ameliorate premature ovarian insufficiency induced by cyclophosphamide in rats and correlate to modulating IL-17A/IL-6 axis and MEK/ERK signals. *J Ethnopharmacol*. 2023;307:116242.
- Pu X, Zhang L, Zhang P, Xu Y, Wang J, Zhao X, et al. Human UC-MSC-derived exosomes facilitate ovarian renovation in rats with chemotherapy-induced premature ovarian insufficiency. *Front Endocrinol*. 2023;14:1205901.
- Yin Y, Li H, Qin Y, Chen T, Zhang Z, Lu G, et al. Moxibustion mitigates mitochondrial dysfunction and NLRP3 inflammatory activation in cyclophosphamide-induced premature ovarian insufficiency rats. *Life Sci*. 2023;314:121283.
- Huang Y, Hu C, Ye H, Luo R, Fu X, Li X, et al. Inflamm-Aging: a new mechanism affecting premature ovarian insufficiency. *J Immunol Res*. 2019;2019:1–7.
- Shelling AN, Ahmed Nasef N. The role of lifestyle and dietary factors in the development of premature ovarian insufficiency. *Antioxid (Basel)*. 2023;12:1601.
- Lliberos C, Liew SH, Zareie P, La Gruta NL, Mansell A, Hutt K. Evaluation of inflammation and follicle depletion during ovarian ageing in mice. *Sci Rep*. 2021;11:278.
- Snider AP, Wood JR. Obesity induces ovarian inflammation and reduces oocyte quality. *Reproduction*. 2019;158:R79–90.
- Rao Z, Zhu Y, Yang P, Chen Z, Xia Y, Qiao C, et al. Pyroptosis in inflammatory diseases and cancer. *Theranostics*. 2022;12:4310–29.
- Fu J, Wu H. Structural mechanisms of NLRP3 Inflammasome Assembly and Activation. *Annu Rev Immunol*. 2023;41:301–16.
- Mangan MSJ, Olhava EJ, Roush WR, Seidel HM, Glick GD, Latz E. Targeting the NLRP3 inflammasome in inflammatory diseases. *Nat Rev Drug Discov*. 2018;17:588–606.
- Chen Y, Miao C, Zhao Y, Yang L, Wang R, Shen D, et al. Inflammasomes in human reproductive diseases. *Mol Hum Reprod*. 2023;29:gaad035.
- Chen Y, Zhao Y, Miao C, Yang L, Wang R, Chen B, et al. Quercetin alleviates cyclophosphamide-induced premature ovarian insufficiency in mice by reducing mitochondrial oxidative stress and pyroptosis in granulosa cells. *J Ovarian Res*. 2022;15:138.
- Navarro-Pando JM, Alcocer-Gómez E, Castejón-Vega B, Navarro-Villarán E, Condés-Hervás M, Mundi-Roldan M, et al. Inhibition of the NLRP3 inflammasome prevents ovarian aging. *Sci Adv*. 2021;7:eabc7409.
- Yoshino J, Baur JA, Imai S, NAD⁺ Intermediates. The Biology and therapeutic potential of NMN and NR. *Cell Metabol*. 2018;27:513–28.
- Loreto A, Antoniou C, Merlini E, Gilley J, Coleman MP. NMN: the NAD precursor at the intersection between axon degeneration and anti-ageing therapies. *Neurosci Res*. 2023;197:18–24.
- Xie N, Zhang L, Gao W, Huang C, Huber PE, Zhou X, et al. NAD⁺ metabolism: pathophysiologic mechanisms and therapeutic potential. *Sig Transduct Target Ther*. 2020;5:227.
- Chu X, Raju RP. Regulation of NAD⁺ metabolism in aging and disease. *Metabolism*. 2022;126:154923.
- Wang L, Chen Y, Wei J, Guo F, Li L, Han Z, et al. Administration of nicotinamide mononucleotide improves oocyte quality of obese mice. *Cell Prolif*. 2022;55:e13303.

Received: 24 June 2024 / Accepted: 9 October 2024

26. Hong W, Mo F, Zhang Z, Huang M, Wei X. Nicotinamide Mononucleotide: a Promising Molecule for Therapy of Diverse diseases by Targeting NAD+ metabolism. *Front Cell Dev Biol.* 2020;8:246.
27. Fu X, He Y, Wang X, Peng D, Chen X, Li X, et al. Overexpression of miR-21 in stem cells improves ovarian structure and function in rats with chemotherapy-induced ovarian damage by targeting PDCD4 and PTEN to inhibit granulosa cell apoptosis. *Stem Cell Res Ther.* 2017;8:187.
28. Marcondes FK, Bianchi FJ, Tanno AP. Determination of the estrous cycle phases of rats: some helpful considerations. *Braz J Biol.* 2002;62:609–14.
29. Cora MC, Kooistra L, Travlos G. Vaginal cytology of the Laboratory Rat and mouse: review and criteria for the staging of the Estrous Cycle using stained vaginal smears. *Toxicol Pathol.* 2015;43:776–93.
30. Adhikari D, Busayavalasa K, Zhang J, Hu M, Risal S, Bayazit MB, et al. Inhibitory phosphorylation of Cdk1 mediates prolonged prophase I arrest in female germ cells and is essential for female reproductive lifespan. *Cell Res.* 2016;26:1212–25.
31. Myers M, Britt KL, Wreford NGM, Ebling FJP, Kerr JB. Methods for quantifying follicular numbers within the mouse ovary. *Reproduction.* 2004;127:569–80.
32. Han C, Yang Y, Guan Q, Zhang X, Shen H, Sheng Y, et al. New mechanism of nerve injury in Alzheimer's disease: β -amyloid-induced neuronal pyroptosis. *J Cell Mol Med.* 2020;24:8078–90.
33. Liu Q, Su L-Y, Sun C, Jiao L, Miao Y, Xu M, et al. Melatonin alleviates morphine analgesic tolerance in mice by decreasing NLRP3 inflammasome activation. *Redox Biol.* 2020;34:101560.
34. Liang A, Zhang W, Wang Q, Huang L, Zhang J, Ma D, et al. Resveratrol regulates insulin resistance to improve the glycolytic pathway by activating SIRT2 in PCOS granulosa cells. *Front Nutr.* 2022;9:1019562.
35. Vincent AJ, Laven JS. Early Menopause/Premature ovarian insufficiency. *Semin Reprod Med.* 2020;38:235–6.
36. Armeni E, Paschou SA, Gouliis DG, Lambrinouadaki I. Hormone therapy regimens for managing the menopause and premature ovarian insufficiency. *Best Pract Res Clin Endocrinol Metab.* 2021;35:101561.
37. Tobias DK, Akinkuolie AO, Chandler PD, Lawler PR, Manson JE, Buring JE, et al. Markers of inflammation and incident breast Cancer risk in the women's Health Study. *Am J Epidemiol.* 2018;187:705–16.
38. Bedoschi G, Navarro PA, Oktay K. Chemotherapy-Induced damage to Ovary: mechanisms and clinical impact. *Future Oncol.* 2016;12:2333–44.
39. Sellami I, Beau I, Sonigo C. Chemotherapy and female fertility. *Ann Endocrinol (Paris).* 2023;84:382–7.
40. Cho H-W, Lee S, Min K-J, Hong JH, Song JY, Lee JK, et al. Advances in the treatment and Prevention of Chemotherapy-Induced ovarian toxicity. *IJMS.* 2020;21:7792.
41. Cohen LE. Cancer Treatment and the Ovary: the effects of Chemotherapy and Radiation. *Ann NY Acad Sci.* 2008;1135:123–5.
42. Salama M, Woodruff TK. Anticancer treatments and female fertility: clinical concerns and role of oncologists in oncofertility practice. *Expert Rev Anticancer Ther.* 2017;17:687–92.
43. Loren AW, Mangu PB, Beck LN, Brennan L, Magdalinski AJ, Partridge AH, et al. Fertility preservation for patients with Cancer: American Society of Clinical Oncology Clinical Practice Guideline Update. *JCO.* 2013;31:2500–10.
44. Li T, Liu J, Liu K, Wang Q, Cao J, Xiao P, et al. Alpha-ketoglutarate ameliorates induced premature ovarian insufficiency in rats by inhibiting apoptosis and upregulating glycolysis. *Reprod Biomed Online.* 2023;46:673–85.
45. Liu M, Zhang D, Zhou X, Duan J, Hu Y, Zhang W, et al. Cell-free fat extract improves ovarian function and fertility in mice with premature ovarian insufficiency. *Stem Cell Res Ther.* 2022;13:320.
46. Xueling L, Kun MA, Wenhua T, Zhongkun XU, Gang L, Chunyan HU, et al. Natural products for treatment of premature ovarian failure: a narrative review. *J Tradit Chin Med.* 2023;43:606–17.
47. Nadeeshani H, Li J, Ying T, Zhang B, Lu J. Nicotinamide mononucleotide (NMN) as an anti-aging health product – promises and safety concerns. *J Adv Res.* 2022;37:267–78.
48. Soma M, Lalam SK. The role of nicotinamide mononucleotide (NMN) in anti-aging, longevity, and its potential for treating chronic conditions. *Mol Biol Rep.* 2022;49:9737–48.
49. Bertoldo MJ, Listijono DR, Ho W-HJ, Riepsamen AH, Goss DM, Richani D, et al. NAD+ repletion rescues female fertility during Reproductive Aging. *Cell Rep.* 2020;30:1670–e16817.
50. Yang Q, Cong L, Wang Y, Luo X, Li H, Wang H, et al. Increasing ovarian NAD+ levels improve mitochondrial functions and reverse ovarian aging. *Free Radic Biol Med.* 2020;156:1–10.
51. Miao Y, Cui Z, Gao Q, Rui R, Xiong B. Nicotinamide Mononucleotide supplementation reverses the declining quality of maternally aged oocytes. *Cell Rep.* 2020;32:107987.
52. Huang P, Zhou Y, Tang W, Ren C, Jiang A, Wang X, et al. Long-term treatment of Nicotinamide Mononucleotide improved age-related diminished ovary reserve through enhancing the mitophagy level of granulosa cells in mice. *J Nutr Biochem.* 2022;101:108911.
53. Arslan NP, Taskin M, Keles ON. Nicotinamide Mononucleotide and Nicotinamide Riboside Reverse ovarian aging in rats Via Rebalancing mitochondrial fission and Fusion mechanisms. *Pharm Res.* 2024;41:921–35.
54. Yan F, Zhao Q, Li Y, Zheng Z, Kong X, Shu C, et al. The role of oxidative stress in ovarian aging: a review. *J Ovarian Res.* 2022;15:100.
55. Stringer JM, Alesi LR, Winship AL, Hutt KJ. Beyond apoptosis: evidence of other regulated cell death pathways in the ovary throughout development and life. *Hum Reprod Update.* 2023;29:434–56.
56. Chen D, Hu N, Xing S, Yang L, Zhang F, Guo S, et al. Placental mesenchymal stem cells ameliorate NLRP3 inflammasome-induced ovarian insufficiency by modulating macrophage M2 polarization. *J Ovarian Res.* 2023;16:58.
57. Chi Y-N, Hai D-M, Ma L, Cui Y-H, Hu H-T, Liu N, et al. Protective effects of leonurine hydrochloride on pyroptosis in premature ovarian insufficiency via regulating NLRP3/GSDMD pathway. *Int Immunopharmacol.* 2023;114:109520.
58. Tabibzadeh S. Signaling pathways and effectors of aging. *Front Biosci (Landmark Ed).* 2021;26:50–96.
59. Cao T, Ni R, Ding W, Ji X, Fan G-C, Zhang Z, et al. Nicotinamide mononucleotide as a therapeutic agent to alleviate multi-organ failure in sepsis. *J Transl Med.* 2023;21:883.
60. Huang P, Wang X, Wang S, Wu Z, Zhou Z, Shao G, et al. Treatment of inflammatory bowel disease: potential effect of NMN on intestinal barrier and gut microbiota. *Curr Res Food Sci.* 2022;5:1403–11.
61. Liang H, Gao J, Zhang C, Li C, Wang Q, Fan J, et al. Nicotinamide mononucleotide alleviates aluminum induced bone loss by inhibiting the TXNIP-NLRP3 inflammasome. *Toxicol Appl Pharmacol.* 2019;362:20–7.
62. Wang Y, Yang J, Hong T, Chen X, Cui L. SIRT2: controversy and multiple roles in disease and physiology. *Ageing Res Rev.* 2019;55:100961.
63. Zhu C, Dong X, Wang X, Zheng Y, Qiu J, Peng Y, et al. Multiple roles of SIRT2 in regulating physiological and Pathological Signal Transduction. *Genet Res (Camb).* 2022;2022:9282484.
64. Zhang J, Hong Y, Cao W, Yin S, Shi H, Ying W. SIRT2, ERK and Nrf2 mediate NAD+ treatment-Induced increase in the antioxidant capacity of PC12 cells under basal conditions. *Front Mol Neurosci.* 2019;12:108.
65. He M, Chiang H-H, Luo H, Zheng Z, Qiao Q, Wang L, et al. An Acetylation switch of the NLRP3 Inflammasome regulates Aging-Associated chronic inflammation and insulin resistance. *Cell Metab.* 2020;31:580–e5915.
66. Sun X, Duan J, Gong C, Feng Y, Hu J, Gu R, et al. Colchicine ameliorates dilated Cardiomyopathy Via SIRT2-Mediated suppression of NLRP3 inflammasome activation. *J Am Heart Assoc.* 2022;11:e025266.

Publisher's note

Springer Nature remains neutral with regard to jurisdictional claims in published maps and institutional affiliations.